Characterization of Sol-gel Derived Cobalt-doped Willemite via 2D Correlation Spectroscopy

F. Brleković,* K. Mužina, and S. Kurajica
University of Zagreb, Faculty of Chemical Engineering and Technology, Marulićev trg 19, HR 10000 Zagreb, Croatia

doi: https://doi.org/10.15255/CABEQ.2023.2189

Original scientific paper
Received: February 15, 2023
Accepted: May 24, 2023

Cobalt blue is one of the world's most famous blue pigments, but it presents a threat to human health since it is toxic when inhaled or ingested. A safer and environmentally preferable way of obtaining cobalt blue-like pigments is doping of various nontoxic compounds with small amounts of cobalt. In this work, doping of zinc silicate (willemite, Zn_2SiO_4) was carried out with 5, 10, and 15 mol% of Co with the aim of obtaining $Zn_{2-x}Co_xSiO_4$ solid solution. Thermal properties of sol-gel derived samples were examined with simultaneous differential thermal and thermogravimetric analysis (DTA/TGA), which showed dehydration, decomposition, and burning effects, accompanied with mass loss and willemite crystallization effect at 800 °C. X-ray powder diffraction analysis (XRD) indicated the formation of willemite phase at 800 °C, accompanied with ZnO phase and increase in willemite crystallinity with annealing temperature rise from 800 to 1100 °C. Fourier transform infrared spectroscopy (FTIR) showed characteristic bands for present oxides and their bonds along with adsorbed water and carbon dioxide. Colouration of prepared samples changed with annealing temperature, whereas higher Co concentrations and temperatures accentuated the intense blue colour. Diffuse reflectance spectroscopy (DRS) revealed an increase in absorbance with annealing temperature and specific bands as a result of different Co coordination present in the samples. The 2D correlation analysis of FTIR and UV-Vis spectra of the samples thermally treated at various temperatures was utilized to investigate and correlate the changes in the structure with the rise of the annealing temperature. The obtained correlation facilitated the finding of optimal process parameters for the desired pigment quality.

Keywords
willemite, doping, 2D correlation analysis

Introduction

Zinc silicate (Zn_2SiO_4) naturally occurs as the mineral willemite, of the nesosilicate group. The structure of the mineral is composed of tetrahedron framework with zinc and silicon ions occupying tetrahedral sites.[1] Willemite-based ceramics are widely used due to their good mechanical, optical, thermal, and electric properties.[2] Consequently, one of the prominent applications of willemite-based ceramics was in the first-generation fluorescent tube phosphors due to the broad white emission band in Mn-doped willemite.[3] Even though it was replaced by second-generation phosphors, it found new applications, e.g., as luminescent material in different display devices. In addition to Mn doping, willemite has proved to be a good host matrix for a wide range of different rare earth and transition metal ions, which results in a palette of materials with specific applications.[2,4–6]

Throughout mankind's use of pigments, the traditional source of blue colour in ceramic pigments was the cobalt ion present in two different minerals – cobalt aluminate or cobalt spinel ($CoAl_2O_4$) and cobalt silicate or cobalt olivine (Co_2SiO_4). Due to its spinel structure, $CoAl_2O_4$ has the ability of tuning the colour to a greener shade, and – compared to cobalt olivine – it possesses half the amount of cobalt ions, but both of these pigments can produce a pure navy blue colour.[7] Depending on the oxidation state, coordination number, and host parameters, Co ions give rise to a set of different colours in the doped material. Octahedral coordination electronic transitions of Co^{3+} ions result in a green colour, and that of Co^{2+} ions in pink to violet, while electronic transitions of Co^{2+} ions in tetrahedral coordination give rise to a blue colour.[8] Despite its established use in ceramic pigments, cobalt is a scarce and expensive element, toxic for humans and harmful to the environment. Consequently, the everyday use of cobalt should be reduced, and one

*Corresponding author: Filip Brleković, e-mail: fbrlekovi@fkit.hr

possible way of achieving this goal is the preparation of pigments via doping of different minerals with cobalt.[9] High thermal stability, as well as the aforementioned good host matrix properties, plus satisfying colouration and hue with the use of relatively low cobalt-doping level make willemite a suitable material for cobalt doping. The doping process involves the replacement of Zn^{2+} ions in tetrahedral sites of the Zn_2SiO_4 olivine structure with Co^{2+} ions.[10] Different methods of preparation result in different properties of the Co-doped willemite. Some of the methods used for preparation of cobalt-doped willemite include hydrothermal synthesis,[11] solid-state high temperature sintering,[12,13] solution combustion method,[14] and the sol-gel method.[5,6,14,15] The sol-gel route possesses numerous advantages, such as the possibility of simple and fine tuning of properties of the final product, as well as easily achievable homogeneity of precursors and lower temperature of the final thermal treatment in comparison to other methods,[5,16] which is why it is the method of choice in many cobalt-doped willemite investigations,[5,6,15] as well as this work.

Two-dimensional correlation (2D-corr) or, more precisely, generalized two-dimensional correlation is a very flexible technique for the analysis of a group of spectroscopic data of a system under the influence of outer perturbation. The external change can be in a time domain or it can be some other type of impulse that initiates the change, such as temperature of annealing, pH change, addition of reactants and their concentration, pressure or their combination.[17,18] This type of analysis is traditionally used on results from different spectroscopic methods, such as nuclear magnetic resonance spectroscopy (NMR), Fourier transformation infrared spectroscopy, near infrared spectroscopy (NIR), UV-Vis spectroscopy, etc. The new generations of 2D-corr analysis have extended the scope of applicable methods to methods like X-ray powder diffraction or mass spectroscopy.[19,20] Main results of 2D-corr analysis are two spectra, synchronous and asynchronous, both containing information in their intensities as a quantitative measure of resemblance or difference of spectral variables. Intensities of the synchronous and asynchronous spectra are obtained by correlation of two measured distinct spectral variables, v_1 and v_2. Furthermore, these measured spectral variables are two different values from the same spectra of the measured data, and they are correlated throughout their change induced by the external perturbation. Synchronous 2D correlation spectrum contains information about concurrent or coincidental changes of two different spectral intensities variations measured at v_1 and v_2 during the external perturbation. The intensities of the asynchronous spectrum indicate sequential or subsequent change in spectral intensities measured independently at v_1 and v_2 with the same external perturbation. Thus, while synchronous correlation spectrum points provide information on coincidental changes, the asynchronous spectrum correlation indicates a non-coincidental change.[21,22] Here it is important to note that, although the names synchronous and asynchronous spectrum are traditionally used, which imply temporal perturbation, the character of the perturbation does not have to be temporal.

In this work, pure and 5, 10, and 15 mol% Co-doped willemite samples were synthesized via the sol-gel route and thermally treated for 2 hours at temperatures ranging from 800 to 1100 °C with the step of 100 °C. The as-prepared and thermally treated samples were characterized by simultaneous differential thermal analysis and thermogravimetric analysis (DTA/TGA), X-ray diffraction (XRD), UV-Vis diffuse reflectance spectroscopy (DRS), and Fourier transform infrared spectroscopy (FTIR). The UV-Vis-DRS and FTIR results were put through 2D correlation analysis to investigate and correlate the changes in the structure with the rise of the annealing temperature.

Materials and methods

Pure and doped willemite samples were synthesized using tetraethyl orthosilicate, TEOS, (p.a., Merck, Germany), $Zn(NO)_2 \cdot 6H_2O$ (p.a., Scharlau, Spain) and $Co(NO_3) \cdot 6H_2O$ (p.a., Merck, Germany) as precursors. Samples with 0, 5, 10, and 15 mol% Co were prepared by separately mixing solutions of 0.025 mol of TEOS and 0.5 mol of ethanol (Gram mol, Croatia), and a solution of nitrate precursors, total 0.05 mol of Zn and Co nitrate, in respect to aforementioned molar percentages, in 1.5 moles of distilled water, and denoted ZC0N, ZC1N, ZC2N and ZC3N, respectively. Both solutions were mixed in an airtight container for an hour to enable the dissolution of precursors and reach maximum homogenization. In the next step, the nitrate solution was added drop by drop into the TEOS solution and mixed for another hour. Diluted ammonia was added to the reaction mixture as a condensation catalyst, after which the solution was mixed for 30 minutes. In the last step, the sol was poured into a large Petri dish and left at room temperature to achieve gel state. Gelation was achieved after 24 hours, and the resulting gel was dried at 45 °C for 2 hours. The dried product was ground into a fine powder and then annealed at temperatures ranging from 800 to 1100 °C.

Dried gels and thermally treated sample's crystallinity and phase composition were determined by

XRD analysis on the Shimadzu XRD 6000 with CuKα radiation in the 2θ range from 10 to 70° with 2θ step of 0.02° and 0.6 s counting time. Thermal properties and behaviour of prepared samples were investigated by simultaneous DTA/TGA analysis using Netzsch STA 409 analyser with a heating rate of 10 °C min^{-1} up to the temperature of 1000 °C. Diffuse reflectance spectra were acquired using Ocean Insight QE Pro High-Performance instrument with an integrating sphere after diluting the samples with barium sulphate (Ba_2SO_4) in a mass ratio of 1:4. Diffuse reflectance was measured in a range from 250 to 900 nm with a spectral resolution of 0.2 nm and an average of 10 spectra. FTIR analysis was carried out on a Bruker Vertex 70 spectrometer in attenuated total reflectance mode (ATR) with samples pressed on a diamond and spectra measured between 400 and 4000 cm^{-1} with a spectral resolution of 2 cm^{-1} and average of 32 scans. 2D correlation analysis calculations and plotting for obtaining synchronous and asynchronous spectra were carried out in MATLAB R2010b using user-created script.

Results and discussion

The XRD patterns of dried gels are presented in Fig. 1. While the pure ZC0N sample is virtually completely amorphous, it can be observed that weak diffraction peaks appear. These peaks are a result of precipitation of small amount of zinc nitrate hydroxide hydrate, $Zn(NO_3)(OH) \cdot H_2O$ (ICDD PDF 2 047-0965). With the increase in Co concentration in the doped samples, a higher amount of crystalline phases appears. The identified crystalline phases are cobalt nitrate hydroxide hydrate, $CoNO_3OH \cdot H_2O$

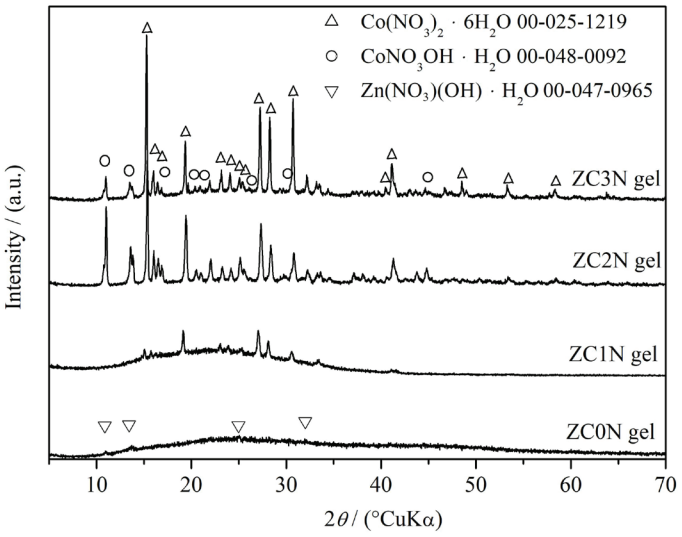

Fig. 1 – *X-ray powder diffraction results of as-prepared samples*

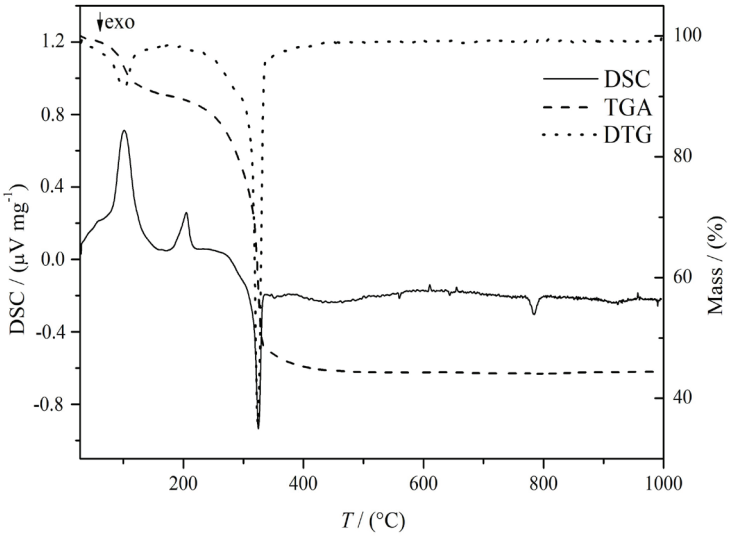

Fig. 2 – *Differential thermal analysis, thermogravimetric analysis, and differential thermogravimetry curves of the as-prepared ZC1N sample*

(ICDD PDF 2 48-0091), and remnant of cobalt precursor, cobalt nitrate hexahydrate, $Co(NO_3)_2 \cdot 6\ H_2O$ (ICDD PDF 2 25-1219). The colour of the formed gels with Co was bright pink, which indicated that there was no change in the oxidation state of the Co ion during the gel synthesis and drying, as it remained in the Co^{2+} state and octahedral coordination.[8]

DTA/TGA analysis (Fig. 2) shows the thermal behaviour of the representative ZC1N sample, since all samples exhibit extremely similar DTA/TGA results. A number of thermal effects can be observed up to 400 °C. First endothermic peak around 100 °C is a direct consequence of water evaporation from the sample, while the second peak at 200 °C is a result of final nitrate decomposition. Exothermic effect present at 350 °C is a convoluted outcome of combustion of different organic remnants in the raw xerogel. Above 400 °C and up to 800 °C the mass becomes constant and there are no more thermal effects, except small artefacts as a result of noise during measurement. At 800 °C, an exothermic peak can be seen, which can be associated with willemite crystallization. Consequently, the samples were thermally treated for 2 hours at temperatures in the range from 800 to 1100 °C to observe and evaluate the formation of willemite and incorporation of Co atoms into its structure.[23,24]

The XRD patterns of the samples treated at 800, 900, 1000, and 1100 °C are presented in Fig. 3. The main phase in all of the samples after annealing at 800 °C is willemite, Zn_2SiO_4 (ICDD PDF 2 37-1485), while zinc oxide, ZnO (ICDD PDF 2 36-1451), crystoballite, SiO_2 (ICDD PDF 2 39-1425) and zinc cobalt oxide, $ZnCo_2O_4$ (ICDD PDF 2 23-1390), are present as secondary phases. These sec-

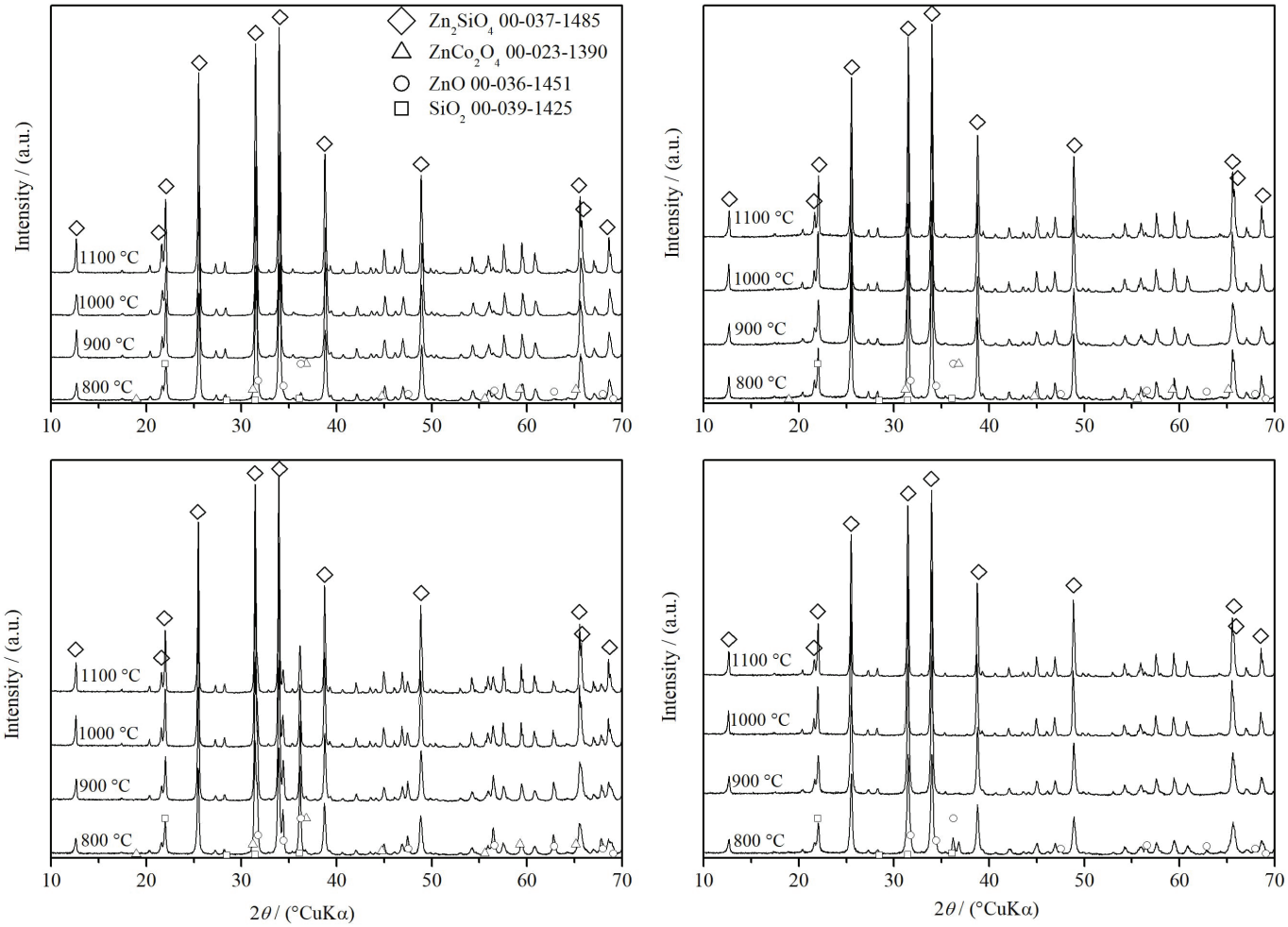

Fig. 3 – *X-ray diffraction patterns of pure and doped willemite samples thermally treated at different temperatures for 2 hours*

ondary phases are the result of the imperfect homogeneity of the gels and precipitation of crystalline nitrate phases with the addition of Co. Zinc cobalt oxide is present only in the sample with the highest Co concentration, which results in the substantially darker shade of blue of the thermally treated ZC3N sample. The crystallinity of all samples increases with the increase in the annealing temperature, as well as the advancement of incorporation of Co and formation of willemite through secondary phases.

FTIR spectra of the thermally treated samples showing the main absorption bands for willemite and similar inorganic compounds in the range from 300 to 1400 cm^{-1} are displayed in Fig. 4. FTIR spectra of the as-prepared samples are not presented due to numerous organic groups' bands. Doped willemite samples show characteristic absorption bands, such as a group of Si–O–M bands, between 800 and 1000 cm^{-1} and absorption bands at 1060 and 460 cm^{-1} related to bending of Si–O bonds in SiO_2 tetrahedron. Two absorption bands around 600 cm^{-1} represent the Zn–O and Co–O bonds. Small bands around 670 cm^{-1} are associated with the 3 or 4 membered silicon-oxygen rings or chain silicate structures in the amorphous phase. It is evident from Fig. 4 that all of the bands develop higher intensities with the rise in annealing temperatures, besides the mentioned absorption bands representing chain structures, which is clearly a consequence of the disappearance of the amorphous phase in favour of more willemite being formed.[25–27]

The UV-Vis diffuse reflectance spectra of all samples annealed at different temperatures are presented in Fig. 5. As-prepared samples exhibit only a wide absorption peak between 400 and 600 nm, which corresponds to the pink colour of the prepared gels due to a Co^{2+} ion in octahedral coordination. In the samples with no added cobalt, the green emission of visible light, i.e., a small peak at 520 nm, is the consequence of UV excitation in willemite which is a natural fluorescent material. The sample with the lowest amount of Co exhibits only a slight difference in spectra obtained at different annealing temperatures. The main group of peaks, the triplet, spanning from 500 to 700 nm is a direct outcome of Co^{2+} transitions in tetrahedral coordination, and gives the desired blue colour to the material. The band centred around 400 nm, which is present

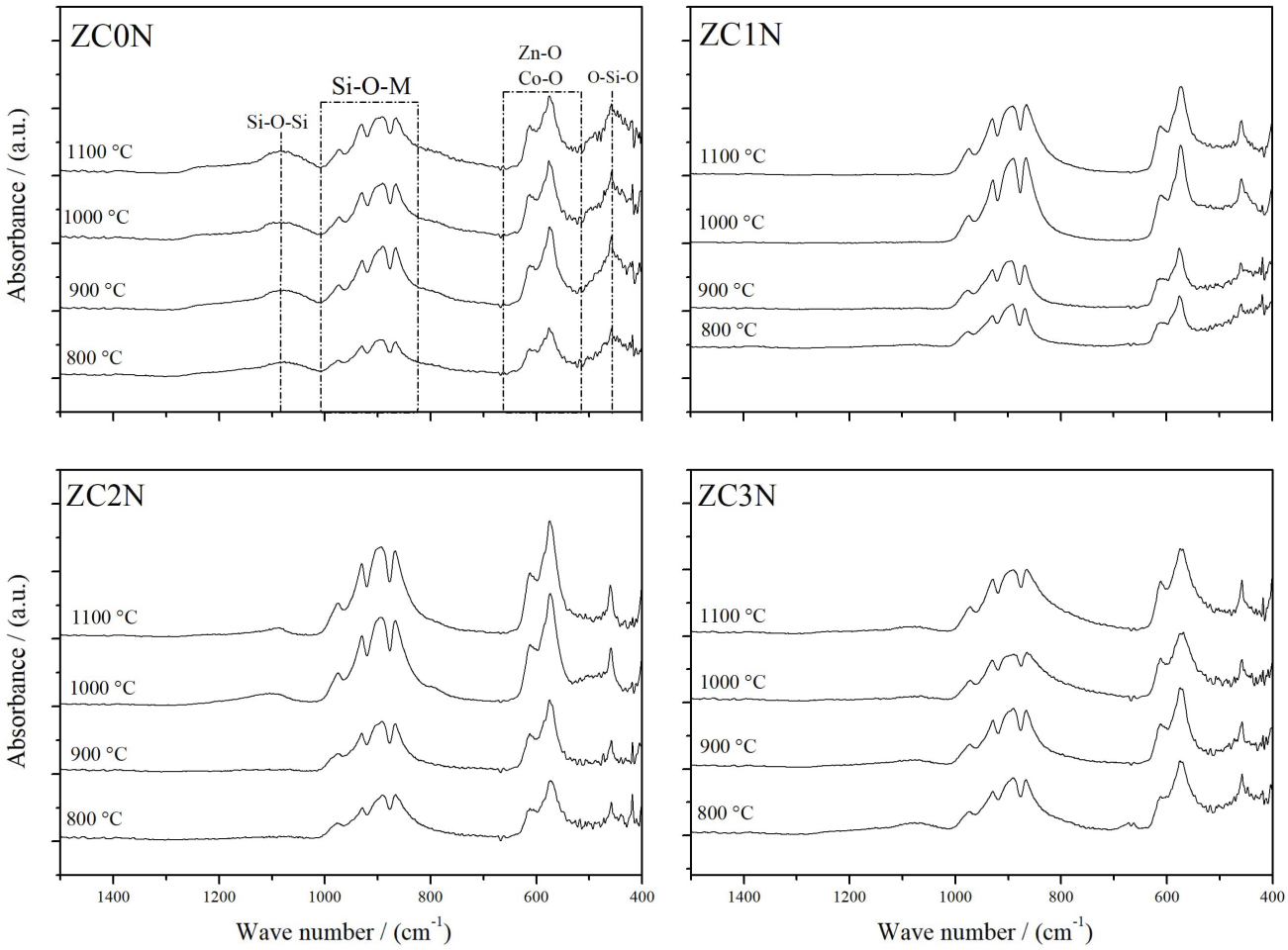

Fig. 4 – *Fourier-transform infrared spectra of all thermally treated samples*

in all samples, indicates the presence of Co^{3+} ions in octahedral coordination. Cobalt ions change to this state when treated between 200 and 700 °C, which gives rise to a greenish hue in samples, visible in ZC1N sample annealed at 800 °C. Similarly, the peak at 460 nm, which can be seen in all doped samples, corresponds to the Co^{2+} ion in octahedral coordination. With the further addition of cobalt to willemite, a new band arises at 720 nm as the product of a new $ZnCo_2O_3$ phase which forms at 800 °C with Co^{3+} in octahedral coordination. This new phase colours the sample in deep and darker shades of blue. With the increase in annealing temperature, the peaks associated to Co^{3+} ions in octahedral coordination lose their intensities in every sample, while the Co^{2+} tetrahedral triplet becomes more prominent.[8,28,29]

In addition to already described FTIR and DRS spectra, the specific peaks and bands for annealed samples, Co ion oxidation state, and structural changes were analysed and correlated using 2D correlation analysis in relation to the annealing temperature. Specific bands of these spectra in this particular system are highly overlapped and their change with the thermal treatment is not easily grasped. In this instance, the 2D correlation allows for tracking of these elusive changes and states, even when deeply convoluted with other results. Occurrence of different colours arising from the Co ion could be finely tuned with the processing temperature and the doping amount, owing to elucidation of optimal conditions using the correlation graphs.

As previously mentioned, the 2D correlation analysis is a powerful tool which can give insight into the dependence and sequence of change in a system with respect to an outer perturbation. Fig. 6 shows the synchronous and asynchronous spectra of non-doped ZC0N sample and 15 mol% Co-doped ZC3N sample. Values on the x axis represent the spectral variable v_1 and y axis the spectral variable v_2, where both of these spectral variables are the wavenumber values from FTIR spectra. Among synchronous correlations, as well as among asynchronous correlations of various samples, no drastic difference could be observed, which is directly related to the similarity of the FTIR spectra of all samples, as may be seen in Fig. 4. Due to this fact, only samples with 0 and 15 % of Co FTIR 2D correlation analysis are shown.

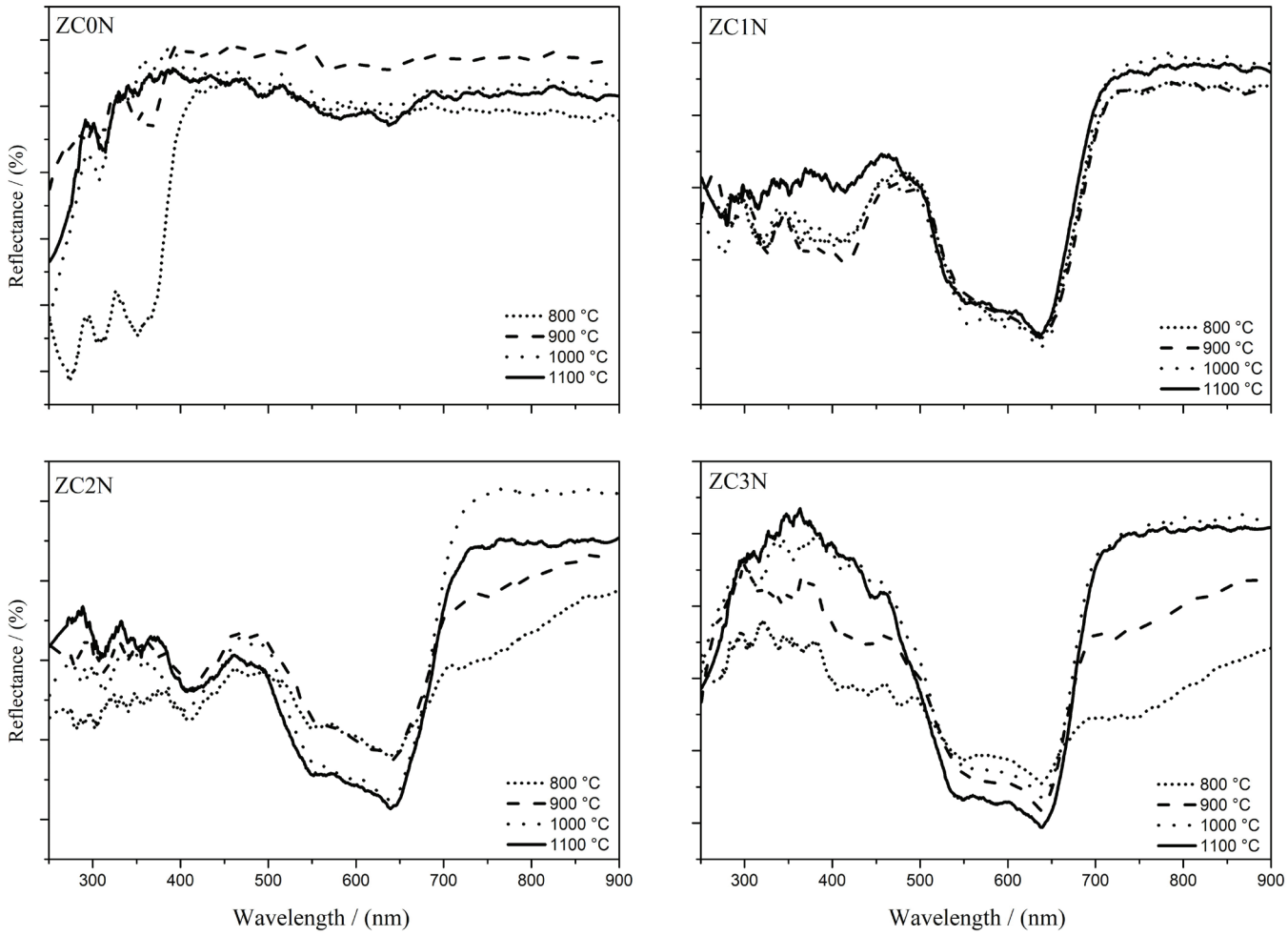

Fig. 5 – *Ultraviolet-visible diffuse reflectance spectra of all thermally treated samples*

To determine the dependence and sequence of changes in the samples, the first step is to analyse the autopeaks. These types of features form only in the synchronous spectrum, and are located on the diagonal of the spectrum. In Fig. 6a and 6c, some strong and some weak autopeaks for the aforementioned specific bands are present. The intensity of the autopeak indicates the magnitude of the change of spectral variable in the spectra with outer perturbation, i.e., the absorption bands around 600 cm^{-1}, arising from Zn–O and Co–O bonds, in Fig. 4 can be clearly seen as having their absorbance elevated and shapes sharpened with the rise in annealing temperature, and this effect is represented as a diagonal peak with substantial intensity values in the synchronous spectra, Fig. 6a and 6c. Furthermore, bands centred around 900 cm^{-1} as a result of Si–O–M bonds also show diagonal peaks of high intensities, which indicates a strong change of these bands with the annealing temperature, while bonds represented at 1060 and 460 cm^{-1} related to bending of Si–O and absorption bands around 670 cm^{-1} associated with the 3 or 4 membered silicon-oxygen rings or chain silicate structures, have weak diagonal peaks pointing to weaker change with the perturbation. All diagonal peaks and bands show crosspeaks (correlation) with each other, which is an indication of simultaneous or coincidental changes – i.e., crosspeaks of two different FTIR spectra bands, one located at 600 cm^{-1} (spectral variable v_1) and other around 900 cm^{-1} (spectral variable v_2), exhibit high positive intensities, which contains the information about the similarity of the direction of change. The information these crosspeaks carry is that the change of both bands is in the same direction. In other words, both of these bands grow stronger with the outer change. Two bands that show negative crosspeaks with all other bands are located around 460 and 670 cm^{-1}. This indicates that the change in intensities of both these bands is opposite to the change in all other bands present in the FTIR spectra.

Crosspeaks are the only feature of the asynchronous spectrum (Fig. 6b and 6d), and they signal the noncoincidental and out-of-phase change of the spectral variables. Due to the high noise to signal ratio, most of the peaks in the range from 400 to 550 cm^{-1} in the asynchronous spectra are either

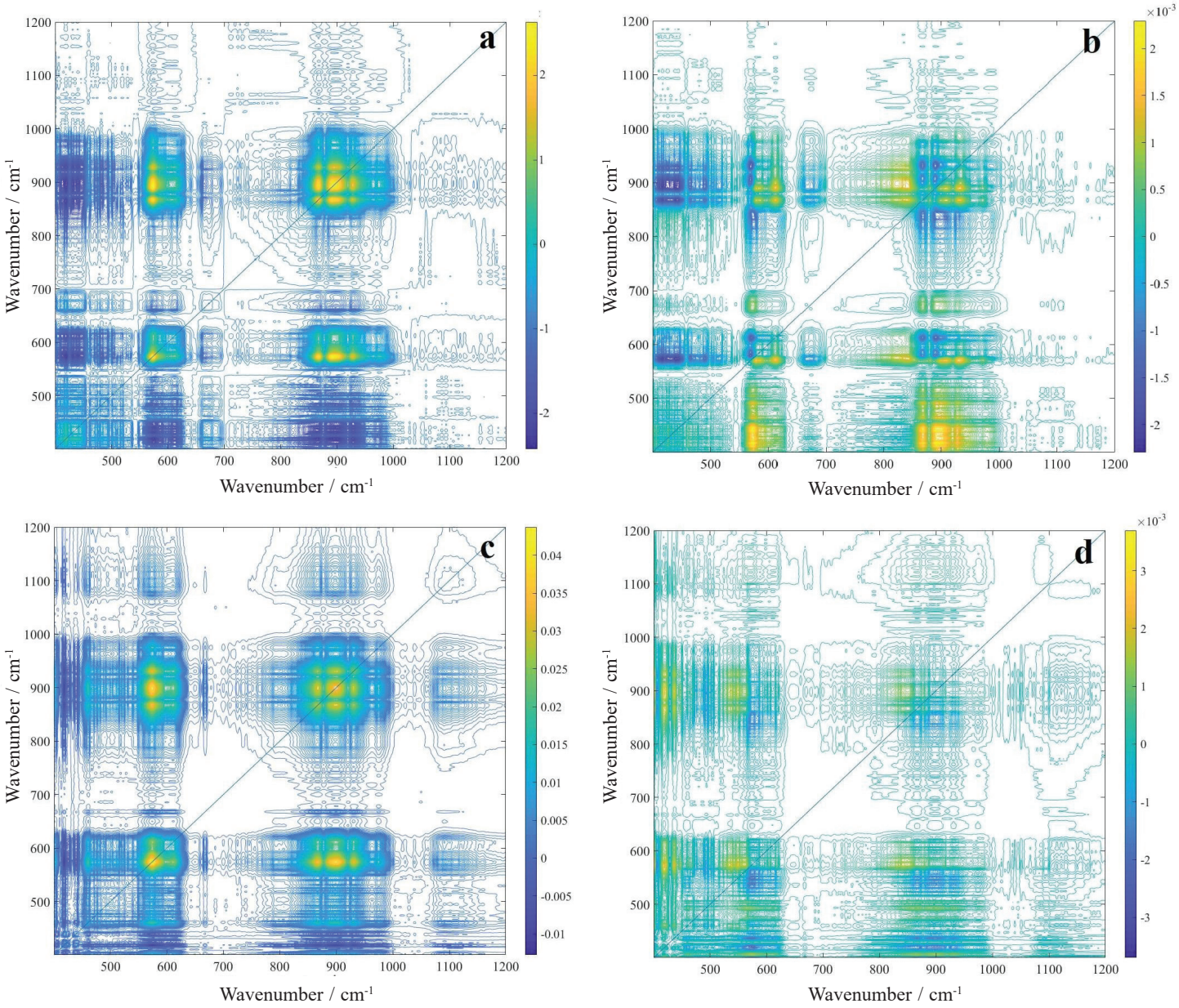

Fig. 6 – *2D correlation synchronous (a) and asynchronous (b) FTIR spectra of ZC0N sample, as well as synchronous (c) and asynchronous (d) FTIR spectra of ZC3N sample*

false crosspeaks or occur due to the sharpening of band at 460 cm^{-1}. Intensities of these peaks are negative, as well as the intensities of their associated peaks in the synchronous spectra, which indicates the opposite value of the peak intensities. This implies that the change at the spectral variable v_1 occurs predominantly before other changes in spectral variable v_2 with which it correlates negatively. Another peak negatively correlating to other peaks is the 670 cm^{-1} peak, which alongside the already mentioned peak has negative synchronous correlation, indicating the preceding change in these bonds to other changes in the system with the outer perturbation. The band around 600 cm^{-1} is composed of two peaks, out of which the peak at 570 cm^{-1} has negative crosspeaks and its change develops after the changes in other bands, and the other peak at 610 cm^{-1} has positive correlation and its changes developed before other changes in the FTIR spectra with the increase in annealing temperature. The bands around 900 cm^{-1} and their correlation to other peaks in the FTIR spectra has been already defined, but the intrinsic correlation is not of great importance as they fundamentally originate from the same effect in the defined Si–O–M bonds. The 1060 cm^{-1} band shows no significant change and no strong correlation to other peaks.

The main conclusions that can be reached from the FTIR 2D correlation analysis is that the bands that are a result of the organized willemite structure have strong synchronous autopeaks, which suggests a great change in the structure and bonds with the

annealing temperature change. Entirety of the bands present in the FTIR spectrum exhibit correlation in both synchronous and asynchronous spectra with one another, which shows that all of the changes in this system are connected. The peaks from the unordered amorphous structure of the precursor gels show negative synchronous and asynchronous correlation to the rest of the spectrum. Therefore, it can be concluded that the amorphous phase is being used to build up the more ordered willemite structure with the rise in annealing temperature.

Since there are no changes in the UV-Vis radiation absorption in pure willemite samples, the UV-Vis DRS 2D correlation analysis will be described only on Co-doped willemite samples.

Willemite absorbs UV radiation, which is evident in the DRS spectra as a sharp decline in the reflectance. 2D correlation algorithm assumes this absorption interval as a peak and correlates it to the rest of the spectrum, and that is why the correlation of lower wavelengths will not be discussed further. The main peaks of interest in this analysis are the

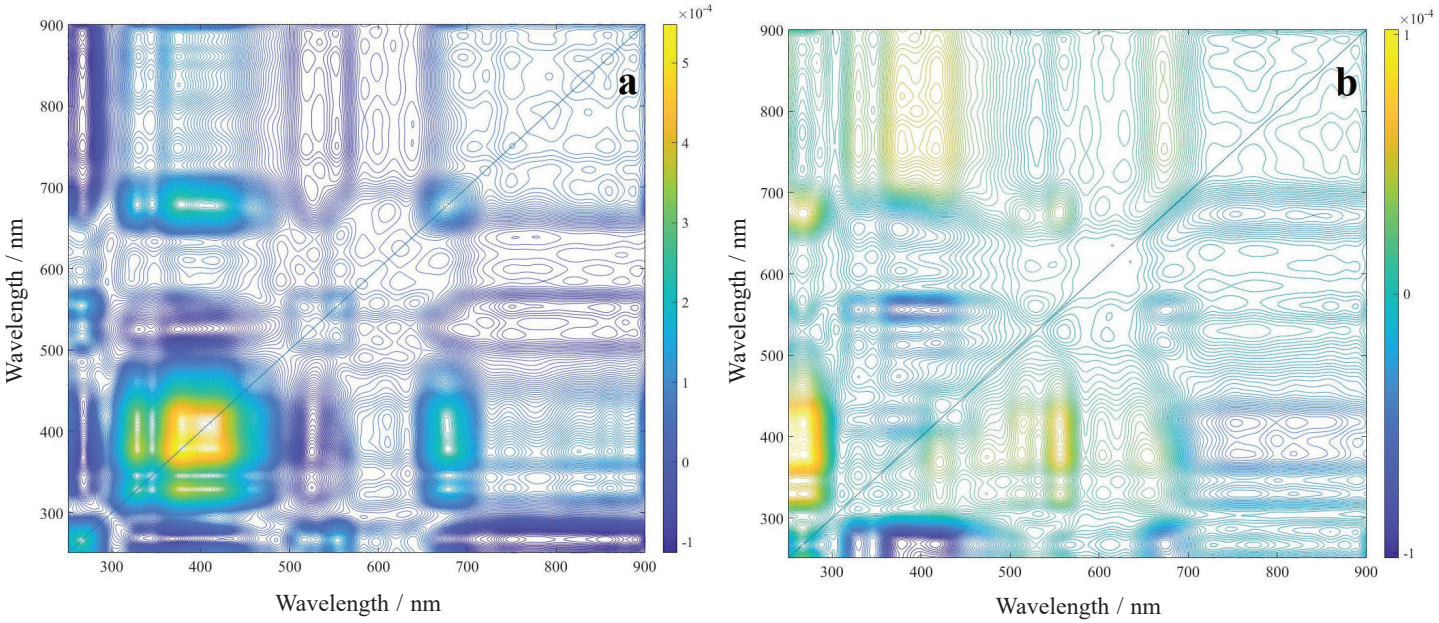

Fig. 7 – *2D correlation synchronous (a) and asynchronous (b) UV-Vis DRS spectra of ZC1N sample*

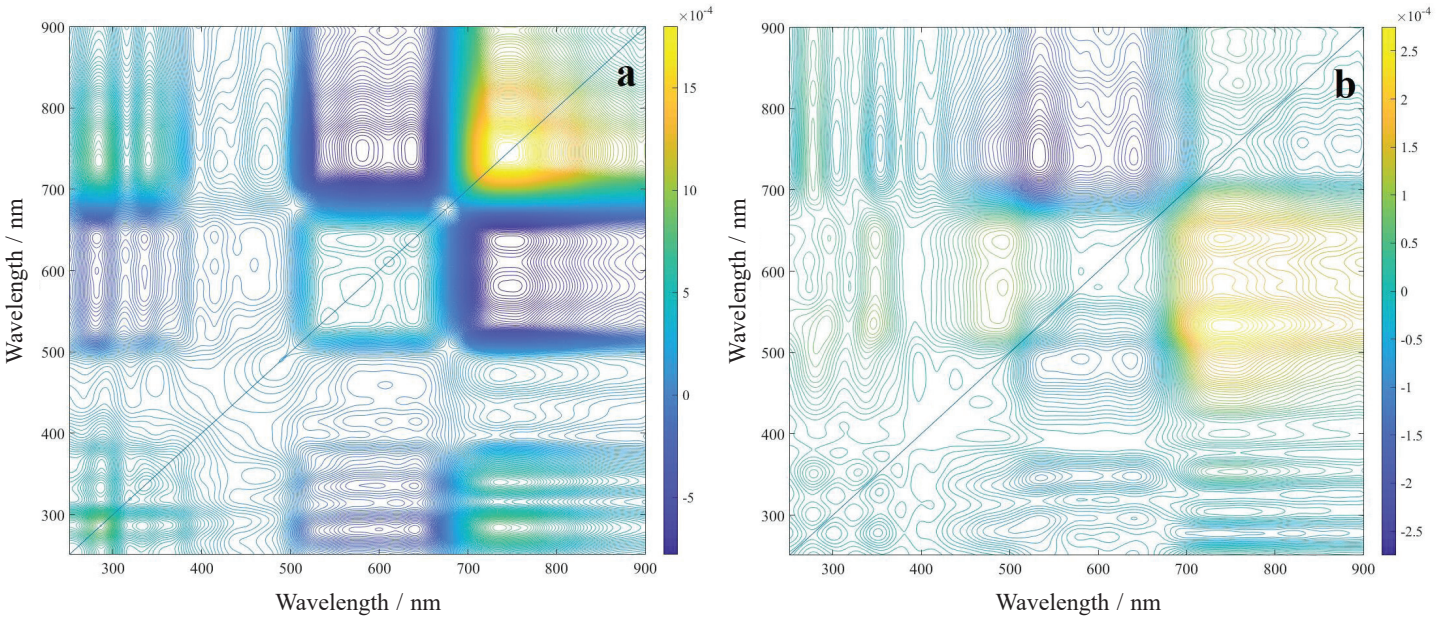

Fig. 8 – *2D correlation synchronous (a) and asynchronous (b) UV-Vis DRS spectra of ZC2N sample*

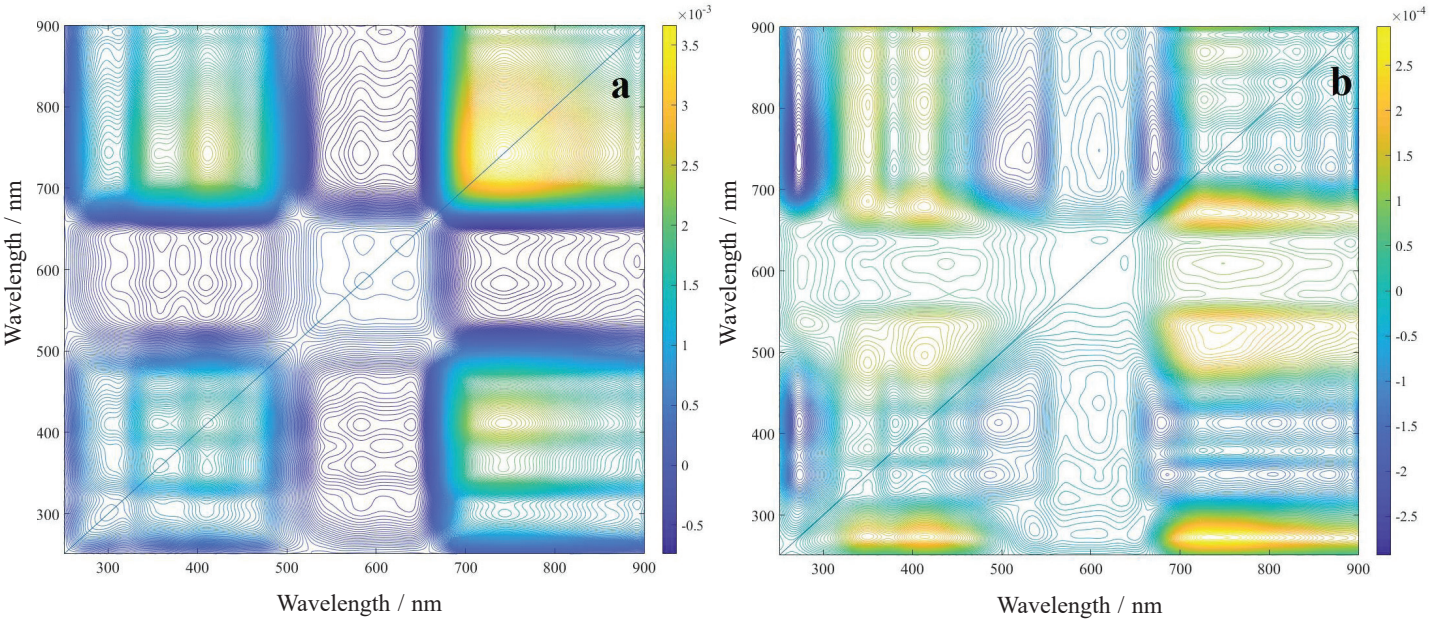

Fig. 9 – *2D correlation synchronous (a) and asynchronous (b) UV-Vis DRS spectra of ZC3N sample*

triplet at 600 nm, the band around 400 nm, and the peak at 720 nm.

By observing the synchronous spectrum, it can be concluded that the 400 nm band has the strongest autopeak, which implies the greatest change with annealing temperature. The triplet shows small autopeak intensities, but only negative correlation with the rest of the spectral variables, while the 720 nm autopeak has average intensity values. This indicates that the change of the triplet with the outer perturbation is modest, and that the change in intensities compared to the other two bands is in the opposite direction (Fig. 7). The asynchronous correlation shows that all the defined peaks are related, and the source of the change with the perturbation is mutual. The triplet correlates positively with the other two bands, but taking into consideration the rule that, if the correlation in the synchronous spectrum is negative, the correlation in the asynchronous spectrum changes values, the result is the negative correlation of the triplet to 400 and 720 nm peaks. This implies that the change of these two peaks occurs predominantly before the changes in the triplet. This correlation points out that the change that happens with the annealing of the doped willemite samples is as follows: with the increase in annealing temperature, the less-desired phases with Co ion in unfavourable states and coordinations disappear in favour of the formation of the doped willemite phase.

Correlation spectra of 10 mol% Co-doped samples show no difference in the correlation of the spectral variables, but there is a difference in the intensities of the correlation peaks. The change in the 720 nm peak is significant, and its correlation to the rest of the spectra is stronger (Fig. 8). This could indicate that the majority of the Co ions that did not get incorporated into the willemite structure at 800 °C are present in the Co^{3+} state and octahedral coordination.[28]

ZC3N sample shows the same correlation in the UV-Vis DRS 2D correlation spectra as the two previous examples, and in the similar manner as the ZC2N sample, i.e., it has highest autopeak at 720 nm in the synchronous spectrum (Fig. 9). This sample appeared extremely dark, almost black, annealed at 800 °C, with additional zinc cobalt oxide phase, in which the Co ion takes octahedral positions and 3+ oxidation state, while the ZC1N sample appeared light green at lower temperatures, which can be ascribed to more Co^{2+} ion in octahedral state. This effect of extreme dark colouration occurred as a result of high doping amount. Namely, a high concentration of cobalt ions in all available oxidation states absorbs light in almost the entire visible range of the electromagnetic spectrum. 2D correlation shows that all of the features seen in UV-Vis DRS spectra, besides the triplet, lose their significance with the annealing temperature increase and that the intensities of the triplet increase at the expense of the other bands present in the spectra.

The information obtained by 2D correlation analysis could be used to achieve the stable pigments of desired colour and hue: teal and light green is achieved with lower temperatures and concentrations of Co doping, darker shade of blue colour resulting from high amount of Co ions in different states annealed at lower temperatures, and finally, stable, intense, and low Co concentration gives blue ceramic pigments.

Conclusions

Sol-gel prepared zinc silicate (Zn_2SiO_4) was successfully doped with 5, 10, and 15 mol% of Co. Untreated samples were composed of amorphous and precipitated nitrate phases whose fraction rose with the amount of Co added. DTA/TGA analysis showed that sol-gel derived willemite had a crystallization temperature around 800 °C. The samples were treated in the range from 800 to 1100 °C, where different temperatures along with different amounts of cobalt doping resulted in various colours and hues. General 2D correlation analysis of FTIR and UV-Vis DRS spectra was employed with the aim of establishing how the change in annealing temperature and cobalt doping affected the structure as well as external properties of the material. Lower temperatures in combination with low amount of Co doping resulted in brighter green colours of prepared pigments, while higher concentrations of Co resulted in darker tones approaching the black colour. With the rise in annealing temperature, all samples achieved cobalt blue-like colour. 2D correlation analysis could facilitate the assessment of optimal process parameters for procuring pigments of desired quality.

ACKNOWLEDGMENT

The aegis of the University of Zagreb is gratefully acknowledged. The authors are grateful to Neven Ukrainczyk, PhD, for the assistance with 2D correlation analysis. Also, thanks to Andrej Terzin for help with the experimental part of this work.

References

1. *Takesue, M., Hayashi, H., Smith Jr., R. L.*, Thermal and chemical methods for producing zinc silicate (willemite): A review, Prog. Cryst. Growth Charact. Mater. **55** (2009) 98. doi: https://doi.org/10.1016/j.pcrysgrow.2009.09.001
2. *Chandra Babu, B., Buddhudu, S.*, Dielectric properties of willemite α-Zn_2SiO_4 nano powders by sol-gel method, Phys. Procedia **49** (2013) 128. doi: https://doi.org/10.1016/j.phpro.2013.10.019
3. *Raymond, K., Sell, H*., Revolution in Lamps: A Chronicle of 50 Years of Progress, Second Edition, River Publishers, Alsbjergvej, 2020, pp 98-120.
4. *Thiyagarajan, P., Kottaisamy, M., Ramachandra Rao, M. S.*, Improved luminescence of Zn_2SiO_4:Mn green phosphor prepared by gel combustion synthesis of ZnO:Mn–SiO_2, J. Electrochem. Soc. **154** (2007) 297. doi: https://doi.org/10.1149/1.2436607
5. *Rasdi, N. M., Fen, Y. W., Azis, R. S., Omar, N. A. S.*, Photoluminescence studies of cobalt (II) doped zinc silicate nanophosphors prepared via sol-gel method, Optik **149** (2017) 409. doi: https://doi.org/10.1016/j.ijleo.2017.09.073
6. *Cui, H., Zayat, M., Levy, D.*, Nanoparticle synthesis of willemite doped with cobalt ions ($Co_{0.05}Zn_{1.95}SiO_4$) by an epoxide-assisted sol−gel method, Chem. Mater. **17** (2005) 5562. doi: https://doi.org/10.1021/cm051289s
7. *Eppler, R. A., Eppler, D. R*., Which color can and cannot be produced in ceramic glazes, Ceram. Eng. Sci. Proc. **15** (1994) 281. doi: https://doi.org/10.1002/9780470314340.ch30
8. *Kurajica, S., Popović, J., Tkalčec, E., Gržeta, B., Mandić, V*., The effect of annealing temperature on the structure and optical properties of sol-gel derived nanocrystalline cobalt aluminate spinel, Mater. Chem. Phys. **135** (2012) 587. doi: https://doi.org/10.1016/j.matchemphys.2012.05.030
9. *Llusar, M., Fores, A., Badenes, J. A., Calbo, J., Tena, M. A., Monros, G.,* Colour analysis of some cobalt-based blue pigments, J. Eur. Ceram. Soc. **21** (2001) 1121. doi: https://doi.org/10.1016/S0955-2219(00)00295-8
10. *Ozel, E., Yurdakul, H., Turan, S., Ardit, M., Cruciani, G., Dondi, M.,* Co-doped willemite ceramic pigments: Technological behaviour, crystal structure and optical properties, J. Eur. Ceram. Soc. **30** (2010) 3319. doi: https://doi.org/10.1016/j.jeurceramsoc.2010.08.013
11. *Pozas, R., Orera, V. M., Ocana, M*., Hydrothermal synthesis of Co-doped willemite powders with controlled particle size and shape, J. Eur. Ceram. Soc. **25** (2005) 3165. doi: https://doi.org/10.1016/j.jeurceramsoc.2004.07.006
12. *Ibreva, T., Dimitrov, T., Titorenkova, R., Markovska, I., Tacheva, E., Petrov, O.,* Synthesis and characterization of willemite ceramic pigments in the system xCoO. (2–x) ZnO. SiO_2, Bulg. Chem. Commun. **50** (2018) 31.
13. *Walaa, M., El-Gawad, A., Abdelmaksoud, W. M.,* Synthesis of eco-friendly cobalt doped willemite blue pigment from white sand for multi-applications in coatings and inks, Pigment. Resin Technol. Vol. ahead-of-print No. ahead-of-print, 2022. doi: https://doi.org/10.1108/PRT-12-2021-0136
14. *Chandrappa, G. T., Ghosh, S., Patil, K. C.*, Synthesis and properties of willemite, Zn_2SiO_4, and M^{2+}:Zn_2SiO_4 (M = Co and Ni), J. Mater. Synth. Process. **7** (1999) 273.
15. *Dimitrov, T. I., Markovska, I. G., Ibreva, T. H.*, The analysis about synthesis, structure and properties of willemite ceramic pigments obtained by a sol–gel method, IOP Conf. Ser. Mater. Sci. Eng. **893** (2020) 012001. doi: https://doi.org/10.1088/1757-899X/893/1/012001
16. *Sajjadi, S. P.*, Sol-gel process and its application in nanotechnology, J. Polym. Eng. **13** (2005) 38.
17. *Harrington, P. de B., Urbas, A., Tandler, P. J.,* Two-dimensional correlation analysis, Chemom. Intell. Lab. Syst. **50** (2000) 149. doi: https://doi.org/10.1016/S0169-7439(99)00062-3
18. *Noda, I.,* Recent advancement in the field of two-dimensional correlation spectroscopy, J. Mol. Struct. **883** (2008) 2. doi: https://doi.org/10.1016/j.molstruc.2007.11.038
19. *Park, Y., Jin, S., Noda, I., Jung, Y. M.,* Emerging developments in two-dimensional correlation spectroscopy (2D-COS), J. Mol. Struct. **1217** (2020) 128405. doi: https://doi.org/10.1016/j.molstruc.2020.128405
20. *Park, Y., Jin, S., Noda, I., Jung, Y. M.,* Continuing progress in the field of two-dimensional correlation spectroscopy (2D-COS): Part III. Versatile applications, Spectrochim. Acta A Mol. Biomol. Spectrosc. **284** (2023) 121636. doi: https://doi.org/10.1016/j.saa.2022.121636
21. *Park, Y., Jin, S., Noda, I., Jung, Y. M.*, Recent progresses in two-dimensional correlation spectroscopy (2D-COS), J. Mol. Struct. **1168** (2018) 1. doi: https://doi.org/10.1016/j.molstruc.2018.04.099

22. *Noda, I.*, Techniques of Two-dimensional (2D) correlation spectroscopy useful in life science research, BSI **4** (2015) 109.
doi: https://doi.org/10.3233/BSI-150105

23. *Malecka, B., Lacz, A., Drozdz, E., Malecki, A.*, Thermal decomposition of d-metal nitrates supported on alumina, J. Therm. Anal. Calorim. **119** (2015) 1053.
doi: https://doi.org/10.1007/s10973-014-4262-9

24. *Kurajica, S., Tkalčec, E., Šipušić, J., Matijašić, G., Brnardić, I., Simčić, I.*, Synthesis and characterization of nanocrystalline zinc aluminate spinel by sol-gel technique using modified alkoxide precursor, J. Sol-Gel Sci. Tech. **46** (2008) 152.
doi: https://doi.org/10.1007/s10971-008-1707-2

25. *Lesniak, M., Partyka, J., Gajek, M., Sitarz, M.*, FTIR and MAS NMR study of the zinc aluminosilicate ceramic glazes, J. Mol. Struct. **1171** (2018) 17.
doi: https://doi.org/10.1016/j.molstruc.2018.05.101

26. *Sitarz, M., Handke, M., Mozgawa, W.*, Identification of silicooxygen rings in SiO_2 based on IR spectra, Spectrochim. Acta A Mol. Biomol. Spectrosc. **56** (2000) 1819.
doi: https://doi.org/10.1016/S1386-1425(00)00241-9

27. *Wang, C., Shaomin, L., Liu, L., Bai, X.*, Synthesis of cobalt–aluminate spinels via glycine chelated precursors, Mater. Chem. Phys. **96** (2006) 361.
doi: https://doi.org/10.1016/j.matchemphys.2005.07.066

28. *Guo, H., Chen, J., Weng, W., Wang, Q., Li, S.*, Facile template-free one-pot fabrication of $ZnCo_2O_4$ microspheres with enhanced photocatalytic activities under visible-light illumination, Chem. Eng. J. **239** (2014) 192.
doi: https://doi.org/10.1016/j.cej.2013.11.021

29. *Liotta, L. F., Pantaleo, G., Macaluso, A., Di Carlo, G., Deganello, G.*, CoO_x catalysts supported on alumina and alumina-baria: Influence of the support on the cobalt species and their activity in NO reduction by C_3H_6 in lean conditions, Appl. Catal. A: Gen. **245** (2003) 167.
doi: https://doi.org/10.1016/S0926-860X(02)00652-X